Plane Wave Integral Representation for Fields in Reverberation Chambers

David A. Hill, *Fellow, IEEE*

***Abstract*— A plane wave integral representation is presented for well-stirred fields in a reverberation chamber. The representation automatically satisfies Maxwell's equations in a source-free region and the statistical properties of the fields are introduced through the angular spectrum, which is taken to be a random variable. Starting with fairly simple and physically appropriate assumptions for the angular spectrum, a number of properties of the electric and magnetic fields and the power received by an antenna or a test object are derived. Many of these properties and test object responses are in agreement with other theories or with measured results. An important result for radiated immunity testing is that the ensemble (stirring) average of received power is equal to the average over plane wave incidence and polarization.**

***Index Terms*— Dipole antenna, electric field, loop antenna, magnetic field, mode-stirred chamber, radiated immunity, reverberation chamber, statistical electromagnetics.**

I. Introduction

REVERBERATION chambers (also called mode-stirred chambers) are experiencing increased use for radiated emissions and immunity measurements. They are electrically large multimoded cavities that use either mechanical stirring [1], [2] or frequency stirring [3], [4] to create a statistically uniform field. Deterministic [5] and statistical [6] mode theories have been used to analyze reverberation chambers, but they are not convenient for predicting the response of the reference antenna or the test object in the chamber environment.

The purpose of this paper is to present a plane-wave, integral representation for the fields that satisfies Maxwell's equations and also includes the statistical properties expected for a well-stirred field. The statistical nature of the fields is introduced through the plane wave coefficients that are taken to be random variables with fairly simple statistical properties. Because the theory uses only propagating plane waves, it is fairly easy to use to calculate the responses of test objects or reference antennas. A less-complete version of this theory has previously been used to derive the spatial correlation function of the fields [7], to derive expressions for chamber Q [8], and to predict the responses of several test objects in reverberation chambers [9]–[11]. However, the complete theory has not been published previously.

Section II presents the basic plane wave integral theory and derivations of important field properties. Section III includes derivations of the responses of antennas or test objects to the statistical field. Section IV derives probability-density functions and further statistical properties of the fields and test object responses. The specific examples of electric and magnetic dipole responses are included in Appendixes A and B.

Manuscript received February 9, 1998; revised May 13, 1998.

The author is with the Electromagnetic Fields Division, National Institute of Standards and Technology, Boulder, CO 80303 USA.

Publisher Item Identifier S 0018-9375(98)06198-5.

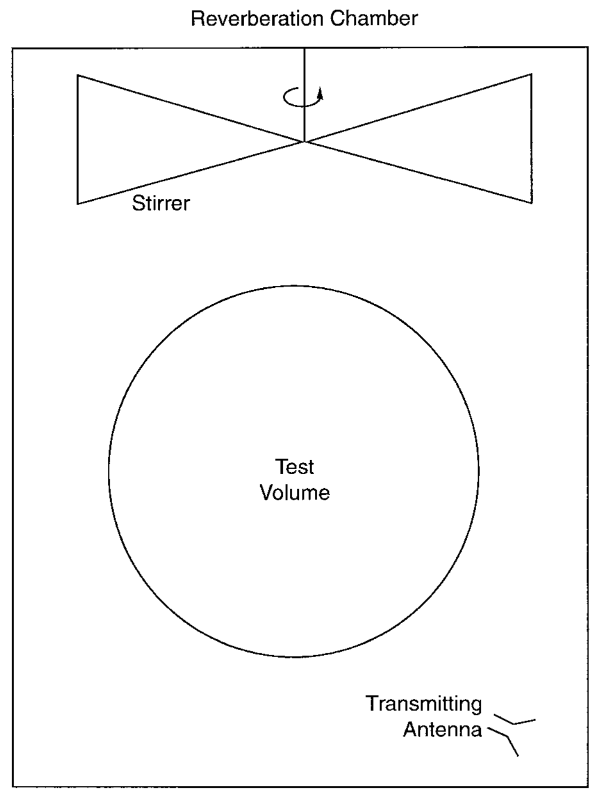

Fig. 1. Test volume in a reverberation chamber with mechanical stirring.

II. Electric and Magnetic Field Properties

A typical geometry for an immunity measurement in a reverberation chamber is shown in Fig. 1. A transmitting antenna radiates CW fields and the mechanical stirrer (or multiple stirrers) is rotated to generate a statistically uniform field. The test volume can occupy a fairly large portion of the chamber volume. The theory presented here applies to single-frequency CW fields that are mechanically stirred; so, it is not directly applicable to frequency stirring.

The electric field $\vec{E}$ at location $\vec{r}$ in a source-free finite volume can be represented as an integral of plane waves over

U.S. Government work not protected by U.S. copyright.

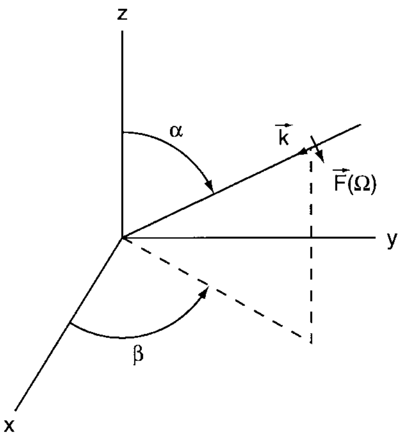

Fig. 2. One vector component $\vec{F}(\Omega)$ of the angular spectrum of the electric field. The wavenumber and the vector component of the angular spectrum are orthogonal.

all real angles [12]

$$\vec{E}(\vec{r}) = \iint_{4\pi} \vec{F}(\Omega) e^{i\vec{k}\cdot\vec{r}}\, d\Omega \tag{1}$$

where the solid angle Ω is shorthand for the elevation and azimuth angles α and β and $d\Omega = \sin\alpha\, d\alpha\, d\beta$. The $\exp(-i\omega t)$ time dependence is suppressed. The vector wavenumber $\vec{k}$ is

$$\vec{k} = -k(\hat{x}\sin\alpha\cos\beta + \hat{y}\sin\alpha\sin\beta + \hat{z}\cos\alpha) \tag{2}$$

where $k = \omega\sqrt{\mu\epsilon}$ is the free-space wavenumber, μ is the free-space permeability, and ϵ is the free-space permittivity. The angular spectrum $\vec{F}(\Omega)$ can be written

$$\vec{F}(\Omega) = \hat{\alpha}F_\alpha(\Omega) + \hat{\beta}F_\beta(\Omega) \tag{3}$$

where $\hat{\alpha}$ and $\hat{\beta}$ are unit vectors that are orthogonal to each other and to $\vec{k}$. Both F_α and F_β are complex and can be written in terms of their real and imaginary parts

$$\begin{aligned} F_\alpha(\Omega) &= F_{\alpha r}(\Omega) + iF_{\alpha i}(\Omega) \quad \text{and} \\ F_\beta(\Omega) &= F_{\beta r}(\Omega) + iF_{\beta i}(\Omega). \end{aligned} \tag{4}$$

The geometry for a plane wave component is shown in Fig. 2.

The electric field in (1) satisfies Maxwell's equations because each plane wave component satisfies Maxwell's equations. For a spherical volume, the representation in (1) can be shown to be complete because it is equivalent to the rigorous spherical-wave expansion [13]. For a nonspherical volume, the plane wave representation can be analytically continued outward from a spherical volume, but the general conditions under which the analytic continuation is valid have yet to be established. In this paper, it is assumed that the volume is selected so that (1) is valid.

For a statistical field as generated in a reverberation chamber, the angular spectrum is taken to be a random variable (which depends on stirrer position). For derivation of many of the important field quantities, the probability-density function of the angular spectrum $\vec{F}(\Omega)$ is not required and it is sufficient to specify certain means and variances. In a typical reverberation chamber measurement, the statistical ensemble is generated by rotating the stirrer (or stirrers). In this paper, $\langle\ \rangle$ represents an ensemble average over stirrer position. The starting point for the statistical analysis is to select statistical properties for the angular spectrum that are representative of a well-stirred field which would be obtained in an electrically large, multimode chamber with a large effective stirrer [2]. Appropriate statistical assumptions for such a field are as follows:

$$\langle F_\alpha(\Omega)\rangle = \langle F_\beta(\Omega)\rangle = 0 \tag{5}$$

$$\begin{aligned} \langle F_{\alpha r}(\Omega_1)F_{\alpha i}(\Omega_2)\rangle &= \langle F_{\beta r}(\Omega_1)F_{\beta i}(\Omega_2)\rangle \\ &= \langle F_{\alpha r}(\Omega_1)F_{\beta r}(\Omega_2)\rangle \\ &= \langle F_{\alpha r}(\Omega_1)F_{\beta i}(\Omega_2)\rangle \\ &= \langle F_{\alpha i}(\Omega_1)F_{\beta r}(\Omega_2)\rangle \\ &= \langle F_{\alpha i}(\Omega_1)F_{\beta i}(\Omega_2)\rangle = 0 \end{aligned} \tag{6}$$

$$\begin{aligned} \langle F_{\alpha r}(\Omega_1)F_{\alpha r}(\Omega_2)\rangle &= \langle F_{\alpha i}(\Omega_1)F_{\alpha i}(\Omega_2)\rangle \\ &= \langle F_{\beta r}(\Omega_1)F_{\beta r}(\Omega_2)\rangle \\ &= \langle F_{\beta i}(\Omega_1)F_{\beta i}(\Omega_2)\rangle \\ &= C_E\delta(\Omega_1 - \Omega_2) \end{aligned} \tag{7}$$

where δ is the Dirac delta function and C_E is a constant with units of $(\mathrm{V/m})^2$.

The mathematical reasons for the assumptions (5)–(7) will become clear when the field properties are derived, but the physical justifications are as follows. Since the angular spectrum is a result of many rays or bounces with random phases, the mean value ought to be zero, as indicated in (5). Since multipath scattering changes the phase and rotates the polarization many times, angular spectrum components with orthogonal polarizations or quadrature phase ought to be uncorrelated, as indicated in (6). Since angular spectrum components arriving from different directions have taken very different multiple scattering paths, they ought to be uncorrelated, as indicated by the delta function on the right side of (7). The coefficient C_E of the delta function is proportional to the square of the electric field strength as will be shown later. The following useful relationships can be derived from (6) and (7):

$$\langle F_\alpha(\Omega_1)F_\beta^*(\Omega_2)\rangle = 0 \tag{8}$$

$$\langle F_\alpha(\Omega_1)F_\alpha^*(\Omega_2)\rangle = \langle F_\beta(\Omega_1)F_\beta^*(\Omega_2)\rangle = 2C_E\delta(\Omega_1 - \Omega_2) \tag{9}$$

where * denotes complex conjugate.

A number of field properties can be derived from (1) and (5)–(9). Consider, first, the mean value of the electric field $\langle\vec{E}\rangle$, which can be derived from (1) and (5):

$$\langle\vec{E}(\vec{r})\rangle = \iint_{4\pi} \langle\vec{F}(\Omega)\rangle e^{i\vec{k}\cdot\vec{r}}\, d\Omega = 0. \tag{10}$$

Thus, the mean value of the electric field is zero because the mean value of the angular spectrum is zero. This result is expected for a well-stirred field, which is the sum of a large number of multipath rays with random phases.

The square of the absolute value of the electric field is important because it is proportional to the electric energy density [10]. From (1), the square of the absolute value of the electric field can be written as a double integral

$$|\vec{\boldsymbol{E}}(\vec{\boldsymbol{r}})|^2 = \iint_{4\pi} \iint_{4\pi} \vec{\boldsymbol{F}}(\Omega_1) \cdot \vec{\boldsymbol{F}}^*(\Omega_2) e^{i(\vec{\boldsymbol{k}}_1 - \vec{\boldsymbol{k}}_2)\cdot\vec{\boldsymbol{r}}}\, d\Omega_1\, d\Omega_2. \tag{11}$$

The mean value of (11) can be derived by applying (8) and (9) to the integrand

$$\langle|\vec{\boldsymbol{E}}(\vec{\boldsymbol{r}})|^2\rangle = 4C_E \iint_{4\pi} \iint_{4\pi} \delta(\Omega_1 - \Omega_2) e^{i(\vec{\boldsymbol{k}}_1 - \vec{\boldsymbol{k}}_2)\cdot\vec{\boldsymbol{r}}} \cdot d\Omega_1\, d\Omega_2. \tag{12}$$

One integration in (12) can be evaluated by using the property of the delta function and the second integration is easily evaluated to obtain the final result

$$\langle|\vec{\boldsymbol{E}}(\vec{\boldsymbol{r}})|^2\rangle = 4C_E \iint_{4\pi} d\Omega_2 = 16\pi C_E \equiv E_0^2. \tag{13}$$

Thus, the mean-square value of the electric field is independent of position. This is the field uniformity property of an ideal reverberation chamber; it applies to the ensemble average of the squared electric field and has been verified experimentally with an array of electric-field probes [2], [14]. For convenience throughout the remainder of the paper, C_E is defined in terms of the mean-square value E_0^2 of the electric field, as indicated in (13).

By a similar derivation, the mean-square values of the rectangular components of the electric field can be derived

$$\langle|E_x|^2\rangle = \langle|E_y|^2\rangle = \langle|E_z|^2\rangle = \frac{E_0^2}{3}. \tag{14}$$

This is the isotropy property of an idealized reverberation chamber, and it has been verified with three-axis electric-field probes [2], [14].

The magnetic field $\vec{\boldsymbol{H}}$ can be derived by applying Maxwell's curl equation to (1)

$$\vec{\boldsymbol{H}}(\vec{\boldsymbol{r}}) = \frac{1}{i\omega\mu}\nabla \times \vec{\boldsymbol{E}}(\vec{\boldsymbol{r}}) = \frac{1}{\eta}\iint_{4\pi} \hat{\boldsymbol{k}} \times \vec{\boldsymbol{F}}(\Omega) e^{i\vec{\boldsymbol{k}}\cdot\vec{\boldsymbol{r}}}\, d\Omega \tag{15}$$

where $\eta = \sqrt{\mu/\epsilon}$ is the free-space impedance. By applying (5)–(15), the mean value of the magnetic field is found to be zero

$$\langle\vec{\boldsymbol{H}}(\vec{\boldsymbol{r}})\rangle = \frac{1}{\eta}\iint_{4\pi} \hat{\boldsymbol{k}} \times \langle\vec{\boldsymbol{F}}(\Omega)\rangle e^{i\vec{\boldsymbol{k}}\cdot\vec{\boldsymbol{r}}}\, d\Omega = 0. \tag{16}$$

The square of the magnitude of the magnetic field can be written as

$$|\vec{\boldsymbol{H}}(\vec{\boldsymbol{r}})|^2 = \frac{1}{\eta^2}\iint_{4\pi} \iint_{4\pi} [\hat{\boldsymbol{k}}_1 \times \vec{\boldsymbol{F}}(\Omega_1)] \cdot [\hat{\boldsymbol{k}}_2 \times \vec{\boldsymbol{F}}^*(\Omega_2)] e^{i(\vec{\boldsymbol{k}}_1 - \vec{\boldsymbol{k}}_2)\cdot\vec{\boldsymbol{r}}}\, d\Omega_1\, d\Omega_2. \tag{17}$$

The derivation of the mean-square value follows closely that of the electric field and the result is

$$\langle|\vec{\boldsymbol{H}}(\vec{\boldsymbol{r}})|^2\rangle = \frac{E_0^2}{\eta^2}. \tag{18}$$

Thus, the mean-square magnetic field also exhibits spatial uniformity and the value is related to the mean-square electric field by the square of the free-space impedance

$$\langle|\vec{\boldsymbol{H}}(\vec{\boldsymbol{r}}_1)|^2\rangle = \frac{\langle|\vec{\boldsymbol{E}}(\vec{\boldsymbol{r}}_2)|^2\rangle}{\eta^2} \tag{19}$$

where $\vec{\boldsymbol{r}}_1$ and $\vec{\boldsymbol{r}}_2$ are arbitrary locations. This free-space relationship has been demonstrated experimentally by using electric and magnetic field probes [2].

The energy density W can be written [15]

$$W(\vec{\boldsymbol{r}}) = \tfrac{1}{2}\,[\epsilon|\vec{\boldsymbol{E}}(\vec{\boldsymbol{r}})|^2 + \mu|\vec{\boldsymbol{H}}(\vec{\boldsymbol{r}})|^2]. \tag{20}$$

The mean value can be obtained from (13), (18), and (20)

$$\langle W(\vec{\boldsymbol{r}})\rangle = \tfrac{1}{2}\,[\epsilon\langle|\vec{\boldsymbol{E}}(\vec{\boldsymbol{r}})|^2\rangle + \mu\langle|\vec{\boldsymbol{H}}(\vec{\boldsymbol{r}})|^2\rangle] = \epsilon E_0^2. \tag{21}$$

Thus, the average value of the energy density is also independent of position. Up to this point, the constant E_0, which was introduced in (7), is arbitrary. However, the theory in [10] can be used to relate E_0 to reverberation chamber quantities via the mean-energy density in (21). From power conservation, the mean energy density can be written [10]

$$\langle W(\vec{\boldsymbol{r}})\rangle = \frac{QP_t}{\omega V} \tag{22}$$

where P_t is the power transmitted into the chamber, Q is the chamber quality factor, and V is the chamber volume. Methods for calculating or measuring Q are given in [10]. From (21) and (22), the following expression for E_0^2 is obtained in terms of chamber parameters:

$$E_0^2 = \frac{QP_t}{\omega\epsilon V}. \tag{23}$$

The power density or Poynting vector $\vec{\boldsymbol{S}}$ can be written [15]

$$\vec{\boldsymbol{S}}(\vec{\boldsymbol{r}}) = \vec{\boldsymbol{E}}(\vec{\boldsymbol{r}}) \times \vec{\boldsymbol{H}}^*(\vec{\boldsymbol{r}}). \tag{24}$$

From (1), (15), and (24), the mean of the power density can be written

$$\langle\vec{\boldsymbol{S}}(\vec{\boldsymbol{r}})\rangle = \frac{1}{\eta}\iint_{4\pi} \iint_{4\pi} \langle\vec{\boldsymbol{F}}(\Omega_1) \times [\hat{\boldsymbol{k}}_2 \times \vec{\boldsymbol{F}}^*(\Omega_2)]\rangle \cdot e^{i(\vec{\boldsymbol{k}}_1 - \vec{\boldsymbol{k}}_2)\cdot\vec{\boldsymbol{r}}}\, d\Omega_1\, d\Omega_2. \tag{25}$$

The expectation in the integrand can be evaluated from vector identities and (8) and (9) as

$$\langle\vec{\boldsymbol{F}}(\Omega_1) \times [\hat{\boldsymbol{k}}_2 \times \vec{\boldsymbol{F}}(\Omega_2)]\rangle = \hat{\boldsymbol{k}}_2 \frac{E_0^2}{4\pi}\delta(\Omega_1 - \Omega_2). \tag{26}$$

The right side of (25) can now be evaluated from (26) and the sampling property of the delta function

$$\langle \vec{S}(\vec{r}) \rangle = \frac{E_0^2}{4\pi\eta} \iint_{4\pi} \hat{k}_2 \, d\Omega_2 = 0. \tag{27}$$

A physical interpretation of (27) is that each plane wave carries equal power in a different direction so that the vector integration over 4π steradians is zero. This result is important because it shows that power density is not the proper quantity for characterizing field strength in reverberation chambers. The mean value of the energy density as given by (21) is an appropriate positive scalar quantity that could be used. Another possibility is to define a positive scalar quantity S that has units of power density and is proportional to the mean energy density

$$S = c\langle W \rangle = \frac{E_0^2}{\eta} \tag{28}$$

where $c = 1/\sqrt{\mu\epsilon}$. For lack of a better term, S will be called scalar power density in the rest of this paper. This quantity could be used to compare with uniform-field plane wave testing, where power density rather than field strength is sometimes specified.

To this point, field properties at a point have been considered. Real antennas and test objects have significant spatial extent and the spatial correlation function of the fields is important in understanding responses of extended objects in reverberation chambers [16]. The spatial correlation function has been derived previously [7], but it will be reviewed briefly here for completeness. The spatial correlation function $\rho(\vec{r}_1, \vec{r}_2)$ of the electric field can be defined as

$$\rho(\vec{r}_1, \vec{r}_2) = \frac{\langle \vec{E}(\vec{r}_1) \cdot \vec{E}^*(\vec{r}_2) \rangle}{\sqrt{\langle (\vec{E}(\vec{r}_1)|^1 \rangle \langle |\vec{E}(\vec{r}_2)|^2 \rangle}} \tag{29}$$

where $\vec{r}_1$ and $\vec{r}_2$ are two arbitrary locations. The numerator of (29) is the mutual coherence function, which has been used to describe wave propagation in random media [17]. The denominator of (29) can be evaluated from (13), and the numerator can be evaluated from (1), (8), and (9) so that the final result is [7]

$$\rho(\vec{r}_1, \vec{r}_2) = \frac{\sin(k|\vec{r}_1 - \vec{r}_2|)}{k|\vec{r}_1 - \vec{r}_2|}. \tag{30}$$

The identical correlation function has been derived from cavity-mode theory [6] and radiative transfer theory [18] and has been checked experimentally [16]. The same correlation function can be derived for the magnetic field and it also applies to acoustic reverberation chambers [19]. A correlation length l_c can be defined as the separation corresponding to the first zero in (30)

$$kl_c = \pi \quad \text{or} \quad l_c = \pi/k = \lambda/2 \tag{31}$$

where λ is the free-space wavelength.

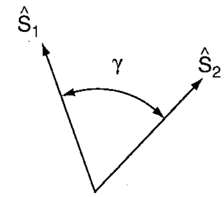

Fig. 3. Unit vectors $\hat{s}_1$ and $\hat{s}_2$ separated by an angle γ.

An angular correlation function $\rho(\hat{s}_1, \hat{s}_2)$ can be defined as

$$\rho(\hat{s}_1, \hat{s}_2) = \frac{\langle E_{s1}(\vec{r}) E_{s2}^*(\vec{r}) \rangle}{\sqrt{\langle |E_{s1}(\vec{r})|^2 \rangle \langle E_{s2}(\vec{r})|^2 \rangle}} \tag{32}$$

where the two electric field components are defined as

$$E_{s1}(\vec{r}) = \hat{s}_1 \cdot \vec{E}(\vec{r}) \quad \text{and} \quad E_{s2}(\vec{r}) = \hat{s}_2 \cdot \vec{E}(\vec{r}) \tag{33}$$

and $\hat{s}_1$ and $\hat{s}_2$ are arbitrary unit vectors separated by an angle γ as shown in Fig. 3. From (14), the denominator of (32) is found to equal $E_0^2/3$. The numerator of (32) is evaluated from (1), (8), and (9) and the result for the angular correlation function is

$$\rho(\hat{s}_1, \hat{s}_2) = \hat{s}_1 \cdot \hat{s}_2 = \cos\gamma. \tag{34}$$

The same angular correlation function can be derived for magnetic field components. Equation (34) shows that the three rectangular components of the electric field are uncorrelated and this is consistent with the theory of Kostas and Boverie [20].

Although the theory in this paper is intended primarily for describing the fields in the test volume where an antenna or test object is located, it has also been found to be useful in deriving an expression for the chamber Q. This application requires that the average energy density in (21) is valid throughout the entire cavity volume V and that the plane wave representation in (1) can be extended to the cavity walls where the appropriate boundary conditions are applied. The boundary condition can be met by using Fresnel reflection coefficients [8] or skin-depth theory [21]. Both approaches agree with the modal theory result for chamber Q [5] when the wall conductivity is large.

III. Antenna or Test-Object Response

Consider now a receiving antenna or a test object placed in the test volume. The simplest case of a lossless impedance-matched antenna will be considered first. The received signal can be written as an integral over incidence angle by analogy with Kerns' plane wave scattering-matrix theory [22]. The received signal could be a current, a voltage, or a waveguide mode coefficient, but the general formulation remains the same. Consider the received signal to be a current I induced in a matched load. For an antenna located at the origin, the current can be written as a dot product of the angular spectrum with a receiving function $\vec{S}_r(\Omega)$ integrated over angle

$$I = \iint_{4\pi} \vec{S}_r(\Omega) \cdot \vec{F}(\Omega)\, d\Omega \tag{35}$$

where the receiving function can be written in terms of two components

$$\vec{S}_r(\Omega) = \hat{\alpha} S_{r\alpha}(\Omega) + \hat{\beta} S_{r\beta}(\Omega). \tag{36}$$

It is assumed that the antenna receiving function in the chamber is the same as in free-space. In general, $S_{r\alpha}$ and $S_{r\beta}$ are complex, so the antenna can have arbitrary polarization such as linear or circular.

The mean value of the current I can be shown to zero from (5) and (35)

$$\langle I \rangle = \iint_{4\pi} \vec{S}_r(\Omega) \cdot \langle \vec{F}(\Omega) \rangle\, d\Omega = 0. \tag{37}$$

The absolute value of the square of the current is important because it is proportional to received power P_r

$$P_r = |I|^2 R_r = R_r \iint_{4\pi} \iint_{4\pi} [\vec{S}_r(\Omega_1) \cdot \vec{F}(\Omega_1)] \cdot [\vec{S}_r^*(\Omega_2) \cdot \vec{F}_r^*(\Omega_2)]\, d\Omega_1\, d\Omega_2 \tag{38}$$

where the radiation resistance R_r of the antenna is also equal to the real part of the matched-load impedance. The mean value of the received power can be determined from (8), (9), and (38)

$$\begin{aligned}\langle P_r \rangle &= \langle |I|^2 \rangle R_r \\ &= \frac{E_0^2}{2} \frac{R_r}{4\pi} \iint_{4\pi} [|S_{r\alpha}(\Omega_2)|^2 + |S_{r\beta}(\Omega_2)|^2]\, d\Omega_2.\end{aligned} \tag{39}$$

The physical interpretation of (39) is that the ensemble average of received power is equal to an average over incidence angle (Ω_2) and polarization α and β components.

The integrand of (39) can be related to the effective area of an isotropic antenna $\lambda^2/4\pi$ and the antenna directivity $D(\Omega_2)$ by

$$\eta R_r [|S_{r\alpha}(\Omega_2)|^2 + |S_{r\beta}(\Omega_2)|^2] = \frac{\lambda^2}{4\pi} D(\Omega_2). \tag{40}$$

Substitution of (40) into (39) yields

$$\langle P_r \rangle = \frac{1}{2} \frac{E_0^2}{\eta} \frac{\lambda^2}{4\pi} \frac{1}{4\pi} \iint_{4\pi} D(\Omega_2)\, d\Omega_2. \tag{41}$$

The integral in (41) is known because the average value of D is one. Thus, the final result for the average received power is

$$\langle P_r \rangle = \frac{1}{2} \frac{E_0^2}{\eta} \frac{\lambda^2}{4\pi}. \tag{42}$$

The physical interpretation of (42) is that the average received power is the product of the average scalar power density E_0^2/η times the effective area $\lambda^2/4\pi$ of an isotropic antenna times a polarization mismatch factor of 1/2 [23]. This result is independent of the antenna directivity and polarization characteristics and is consistent with the reverberation chamber analysis [1] of Corona *et al*. The special cases of an electrically short dipole (electric field probe) and an electrically small loop (magnetic field probe) are discussed in Appendixes A and B.

The preceding analysis can be extended to the case of a real antenna with loss and impedance mismatch by using Tai's theory [23]. The effective area A_e can be generalized to

$$A_e(\Omega) = \frac{\lambda^2}{4\pi} D(\Omega) p m \eta_a \tag{43}$$

where p is the polarization mismatch, m is the impedance mismatch, and η_a is the antenna efficiency. All three quantities—$p, m,$ and η_a—are real and can vary between zero and one. The average of A_e over incidence angle and polarization can be written [23]

$$\langle A_e \rangle = \frac{\lambda^2}{8\pi} m \eta_a. \tag{44}$$

The average received power is

$$\langle P_r \rangle = \frac{E_0^2}{\eta} \langle A_e \rangle \tag{45}$$

where E_0^2/η can again be interpreted as the average scalar power density.

Test objects can be thought of as lossy impedance-mismatched antennas, so (42) also applies to test objects as long as terminals with linear loads can be identified. This theory has been used to predict the responses of an apertured coaxial line [9], an apertured rectangular box [10], and a microstrip transmission line [11] as compared to a reference antenna in a reverberation chamber, and good agreement with measurements has been obtained in each case. Reciprocity can also be applied to this theory to predict the total radiated power in a reverberation chamber and this has been done successfully for the same microstrip transmission line [11].

IV. Probability Density Functions

The statistical assumptions for the angular spectrum in (5)–(7) have been used to derive a number of useful ensemble averages in Sections II and III. These results have not required a knowledge of the particular form of the probability-density functions. However, such knowledge would be very useful for analysis of measured data, which is always based on some limited number of samples (stirrer positions).

The starting point for deriving electric field probability-density functions is to write the rectangular components in terms of their real and imaginary parts

$$\begin{aligned}E_x &= E_{xr} + iE_{xi}, \quad E_y = E_{yr} + iE_{yi}, \\ E_z &= E_{zr} + iE_{zi}.\end{aligned} \tag{46}$$

(The dependence on $\vec{r}$ will be omitted where convenient because all of the results in this section are independent of $\vec{r}$.) The mean value of all the real and imaginary parts in (46) is zero as shown in (10)

$$\langle E_{xr} \rangle = \langle E_{xi} \rangle = \langle E_{yr} \rangle = \langle E_{yi} \rangle = \langle E_{zr} \rangle = \langle E_{zi} \rangle = 0. \tag{47}$$

The variance of the real and imaginary parts can be shown to equal half the result for the complex components in (14)

$$\langle E_{xr}^2\rangle = \langle E_{xi}^2\rangle = \langle E_{yr}^2\rangle = \langle E_{yi}^2\rangle = \langle E_{zr}^2\rangle = \langle E_{zi}^2\rangle = \frac{E_0^2}{6} \equiv \sigma^2. \tag{48}$$

The mean and variance of the real and imaginary parts in (47) and (48) are all of the information that can be derived from the initial statistical assumptions in (5) and (7). However, the maximum entropy method [24], [25] can be used to derive the probability-density functions from (47) and (48). For example, consider E_{xr}. The maximum entropy method selects the probability-density function $f(E_{xr})$ to maximize the entropy given by the integral

$$-\int_{-\infty}^{\infty} f(E_{xr}) \ln[f(E_{xr})]\, dE_{xr} \tag{49}$$

subject to the constraints in (47) and (48) and the usual probability integral constraint

$$\int_{-\infty}^{\infty} f(E_{xr})\, dE_{xr} = 1. \tag{50}$$

The maximization of (49) subject to the constraints (47), (48), and (50) is performed by the method of Lagrange multipliers [25] and the result for f is the normal distribution

$$f(E_{xr}) = \frac{1}{\sqrt{2\pi}\sigma} \exp\left[-\frac{E_{xr}^2}{2\sigma^2}\right] \tag{51}$$

where σ is defined in (48). The same probability-density function also applies to the other real and imaginary parts of the electric field components.

Equations (1), (6), and (7) can be used to show that the real and imaginary parts of the electric field components are uncorrelated. Only the derivation for $\langle E_{xr}E_{xi}\rangle$ will be shown, but the derivations for the other correlations are similar. From (1)–(4), the real and imaginary parts of E_x can be written

$$\begin{aligned} E_{xr}(\vec{r}) = \iint_{4\pi} & \{[\cos\alpha\cos\beta F_{\alpha r}(\Omega) - \sin\beta F_{\beta r}(\Omega)] \\ & \cdot \cos(\vec{k}\cdot\vec{r}) - [\cos\alpha\cos\beta F_{\alpha i}(\Omega) - \sin\beta F_{\beta i}(\Omega)] \\ & \cdot \sin(\vec{k}\cdot\vec{r})\}\, d\Omega \end{aligned} \tag{52}$$

$$\begin{aligned} E_{xi}(\vec{r}) = \iint_{4\pi} & \{[\cos\alpha\cos\beta F_{\alpha i}(\Omega) - \sin\beta F_{\beta i}(\Omega)] \\ & \cdot \cos(\vec{k}\cdot\vec{r}) + [\cos\alpha\cos\beta F_{\alpha r}(\Omega) - \sin\beta F_{\beta r}(\Omega)] \\ & \cdot \sin(\vec{k}\cdot\vec{r})\}\, d\Omega. \end{aligned} \tag{53}$$

The average value of the product of (52) and (53) can be evaluated by using (6) and (7) inside the double integral and making use of the delta function to evaluate one integration. Then the remaining integrand is zero

$$\begin{aligned} \langle E_{xr}(\vec{r})E_{xi}(\vec{r})\rangle = \frac{E_0^2}{16\pi}\iint_{4\pi} & [\cos^2\alpha_2\cos^2\beta_2 + \sin^2\beta_2] \\ & \cdot [\cos(\vec{k}_2\cdot\vec{r})\sin(\vec{k}_2\cdot\vec{r}) \\ & - \cos(\vec{k}_2\cdot\vec{r})\sin(\vec{k}_2\cdot\vec{r})]\, d\Omega_2 = 0. \end{aligned} \tag{54}$$

Similar evaluations show that the real and imaginary parts of all three rectangular components are uncorrelated. Since they are Gaussian, they are also independent [26].

Since the real and imaginary parts of the rectangular components of the electric field have been shown to be normally distributed with zero mean and equal variances and are independent, the probability-density functions of various electric field magnitudes or squared magnitudes are χ or χ-square distributions with the appropriate number of degrees of freedom. The magnitude of any of the electric field components (for example, $|E_x|$) is χ distributed with two degrees of freedom and consequently has a Rayleigh distribution [26]

$$f(|E_x|) = \frac{|E_x|}{\sigma^2} \exp\left[-\frac{|E_x|^2}{2\sigma^2}\right]. \tag{55}$$

The squared magnitude of any of the electric field components (for example, $|E_x|^2$) is chi-square distributed with two degrees of freedom and, consequently, it has an exponential distribution [26]

$$f(|E_x|^2) = \frac{1}{2\sigma^2} \exp\left[-\frac{|E_x|^2}{2\sigma^2}\right]. \tag{56}$$

The probability-density functions in (55) and (56) agree with Kostas and Boverie [20]. They suggest that the exponential distribution in (56) is also applicable to the power received by a small linearly polarized antenna, but it will be shown later that the exponential distribution applies to the power received by any type of antenna.

The total electric field magnitude $|\vec{E}|$ is χ distributed with six degrees of freedom and has the following probability-density function [20], [26]:

$$f(|\vec{E}) = \frac{|\vec{E}|^5}{8\sigma^6} \exp\left[-\frac{|\vec{E}|^2}{2\sigma^2}\right]. \tag{57}$$

The squared magnitude of the total electric field is χ-square distributed with 6° of freedom and has the following probability-density function [26]:

$$f(|\boldsymbol{E}|^2) = \frac{|\vec{E}|^4}{16\sigma^6} \exp\left[-\frac{|\vec{E}|^2}{2\sigma^2}\right]. \tag{58}$$

The dual probability-density functions for the magnetic field can be obtained by starting with the variance of the real or imaginary parts of one of the magnetic field components, for example H_{xr}

$$\langle H_{xr}^2\rangle = \frac{E_0^2}{6\eta_0^2} \equiv \sigma_H^2. \tag{59}$$

Then the dual of the results in (55)–(58) can be obtained by replacing E by H and σ by σ_H.

Similar techniques can be used to analyze the signal received by an antenna. Equation (37) shows that the real and imaginary parts of the current I_r and I_i have zero mean

$$\langle I_r\rangle = \langle I_i\rangle = 0. \tag{60}$$

The derivation of (42) can be modified to obtain the variance of the real and imaginary parts of the current

$$\langle I_r^2 \rangle = \langle I_i^2 \rangle = \frac{1}{4R_r} \frac{E_0^2}{\eta} \frac{\lambda^2}{4\pi} \equiv \sigma_I^2. \tag{61}$$

Since only the mean and variance of the real and imaginary parts of the current are known, the maximum entropy method is again applicable for determining the probability-density function. The result is again the normal distribution for both I_r and I_i

$$f(I_r) = \frac{1}{\sqrt{2\pi}\sigma_I} \exp\left[-\frac{I_r^2}{2\sigma_I^2}\right] \quad \text{and}$$
$$f(I_i) = \frac{1}{\sqrt{2\pi}\sigma_I} \exp\left[-\frac{I_i^2}{2\sigma_I^2}\right]. \tag{62}$$

Equations (6), (7), (35), and (36) can be used to show that I_r and I_i are uncorrelated

$$\langle I_r I_i \rangle = 0. \tag{63}$$

Equations (60)–(63) can be used to show that the current magnitude $|I|$ is χ distributed with two degrees of freedom (Rayleigh distribution)

$$f(|I|) = \frac{|I|}{\sigma_I^2} \exp\left[-\frac{|I|^2}{2\sigma^2}\right]. \tag{64}$$

The current magnitude squared $|I|^2$ is χ-square distributed with two degrees of freedom (exponential distribution)

$$f(|I|^2) = \frac{1}{2\sigma_I^2} \exp\left[-\frac{|I|^2}{2\sigma_I^2}\right]. \tag{65}$$

From (38), the received power P_r is proportional to $I_r^2 + I_i^2$. So P_r is also χ-square distributed with two degrees of freedom and has an exponential probability-density function

$$f(P_r) = \frac{1}{2\sigma_I^2 R_r} \exp\left[-\frac{P_r}{2\sigma_I^2 R_r}\right]. \tag{66}$$

If the load is not matched, then the radiation resistance R_r in (66) is replaced by the load resistance R_l and the expression for σ_I^2 is modified from that given in (61). The result in (66) is in agreement with that of Kostas and Boverie [20], but its derivation is more general. It does not rely on the received power being proportional to the field at a point (such as an electric or magnetic field probe) and is valid for general extended antennas so long as the linearity relationship in (35) holds. The result in (66) has been found to match experimental data in reverberation chambers fairly well for a variety of antennas (dipoles, horns, and log-periodic dipole arrays). The same result is applicable for general test objects as long as they are linear and have identifiable terminals with linear loads.

V. Conclusions

A plane wave integral representation has been presented for well-stirred fields in a reverberation chamber. The representation automatically satisfies Maxwell's equations in a source-free region and the statistical properties are introduced through the angular spectrum, which is taken to be a random variable. Starting with fairly simple and physically appropriate assumptions in (5)–(7), a number of properties of the electric and magnetic fields and the power received by an antenna or a test object have been derived. Many of these properties and test object responses are in agreement with other theories or with measured results. The most important result for testing is that the ensemble (stirring) average of received power is equal to the average over plane wave incidence and polarization [9]–[11]. Consequently, the average responses of receiving antennas or test objects are independent of directivity and polarization properties. By starting with the same simple assumptions in (5)–(7) and applying the maximum entropy method, probability-density functions have been derived for field quantities and received power. These χ and χ-square probability-density functions are consistent with previous results [20] obtained from the central-limit theorem.

The theory in this paper represents an ideal well-stirred case, but some extensions and improvements are needed. This theory applies best to ensemble averages, but most radiated immunity testing uses peak values rather than average values. For a given finite number of samples, the probability-density functions in Section IV can be used to predict peak values and this has worked fairly well for modest numbers of samples. However, these theoretical peak values approach infinity as the number of samples approaches infinity. For quantities such as received power, this is not physically possible. The plane wave integral representation can probably still be used, but the tails of the distribution need some modification to satisfy energy conservation. Another idealization that requires some further attention is the delta function for angular correlation in (7). For real, imperfect stirring, the delta function probably needs to be replaced by a peaked function with some nonzero width. A final point that requires further study is the region of validity of the plane wave integral representation in (1). Even though the expression gives good results when analytically continued outside a spherical source-free region [8], the validity of this analytical continued has not been rigorously demonstrated. Both measurements and theory have a role in resolving all of these issues.

Appendix A
Short Electric Dipole

Consider a short electric dipole of effective length L oriented in the z direction, as shown in Fig. 4. The components $S_{r\alpha}$ and $S_{r\beta}$ of the dipole receiving function are given by

$$S_{r\alpha} = \frac{L \sin\alpha}{2R_r} \quad \text{and} \quad S_{r\beta} = 0 \tag{A.1}$$

where L is the effective length and R_r is the radiation resistance. In (A.1), $S_{r\alpha}$ is derived by dividing the induced voltage by twice the radiation resistance for a matched load. If (A.1) is substituted into (39), the angular integration can be carried out to obtain

$$\langle P_r \rangle = \frac{E_0^2 L^2}{12 R_r}. \tag{A.2}$$

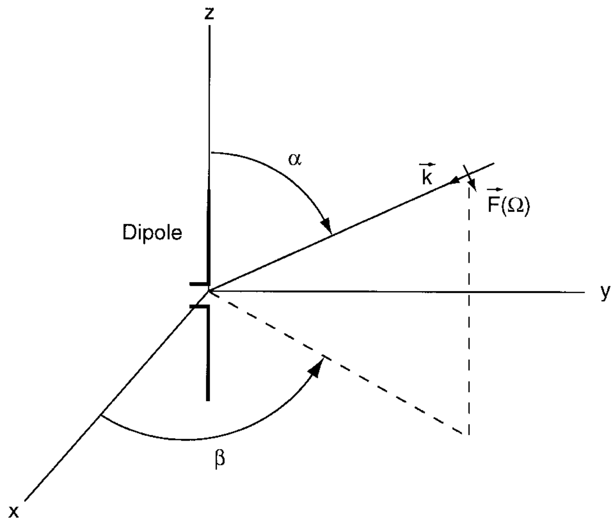

Fig. 4. Short dipole antenna excited by one vector component $\vec{F}(\Omega)$ of the angular spectrum.

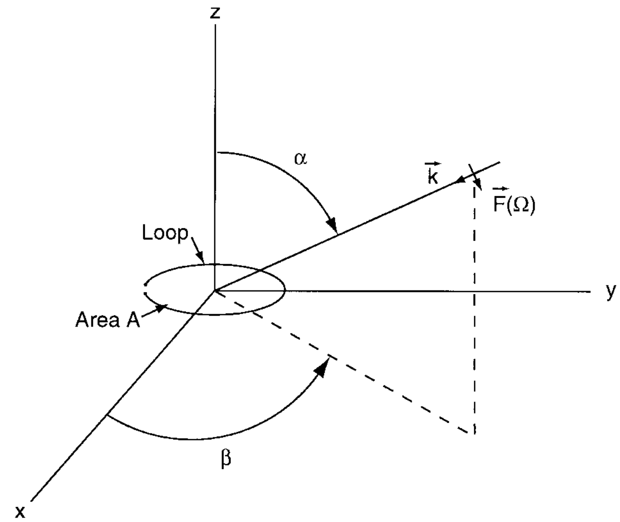

Fig. 5. Small loop antenna excited by one vector component $\vec{F}(\Omega)$ of the angular spectrum.

The radiation resistance of a short electric dipole is [15]

$$R_r = \frac{2\pi\eta L^2}{3\lambda^2}. \tag{A.3}$$

Substitution of (A.3) into (A.2) yields the desired final result

$$\langle P_r \rangle = \frac{1}{2}\frac{E_0^2}{\eta}\frac{\lambda^2}{4\pi} \tag{A.4}$$

which is identical to (42), which was derived for general antennas. The polarization mismatch factor of 1/2 is particularly clear for the electric dipole antenna because $S_{r\beta} = 0$.

Appendix B
Small Loop Antenna

The other electrically small antenna of practical interest is the small loop as shown in Fig. 5. For a small loop of area A centered on the z axis in the xy plane, the components of the receiving function are

$$S_{r\alpha} = 0 \quad \text{and} \quad S_{r\beta} = \frac{-i\omega\mu A \sin\alpha}{2\eta R_r}. \tag{B.1}$$

The results in (B.1) are obtained by: 1) determining the magnetic flux density penetrating the loop; 2) multiplying by $-i\omega$ to determine the induced voltage; and 3) dividing by $2R_r$ to determine the current induced in a matched load. If (B.1) is substituted into (39), the angular integration can be carried out to obtain

$$\langle P_r \rangle = \frac{E_0^2\omega^2\mu^2A^2}{12\eta^2R_r}. \tag{B.2}$$

The radiation resistance of a small loop is [15]

$$R_r = \frac{2\pi\eta}{3}\left(\frac{kA}{\lambda}\right)^2. \tag{B.3}$$

Substitution of (B.3) into (B.2) yields the desired final result

$$\langle P_r \rangle = \frac{1}{2}\frac{E_0^2}{\eta}\frac{\lambda^2}{4\pi} \tag{B.4}$$

which is identical to (42) for general antennas and (A.4) for a short electric dipole. The polarization mismatch factor of 1/2 is also clear for a small loop because $S_{r\alpha} = 0$.

References

[1] P. Corona, G. Latmiral, and E. Paolini, "Performance and analysis of a reverberating enclosure with variable geometry," *IEEE Trans. Electromagn. Compat.*, vol. EMC-22, pp. 2–5, Feb. 1980.

[2] M. L. Crawford and G. H. Koepke, "Design, evaluation, and use of a reverberation chamber for performing electromagnetic susceptibility/vulnerability measurements," U.S. Nat. Bur. Stand. Tech. Note 1092, 1986.

[3] T. A. Loughry, "Frequency stirring: An alternate approach to mechanical mode-stirring for the conduct of electromagnetic susceptibility testing," Phillips Lab., Tech. Rep. PL- TR-91-1036, 1991.

[4] D. A. Hill, "Electronic mode stirring for reverberation chambers," *IEEE Trans. Electromagn. Compat.*, vol. 36, pp. 294–299, Nov. 1994.

[5] B. H. Liu, D. C. Chang, and M. T. Ma, "Eigenmodes and the composite quality factor of a reverberating chamber," U.S. Nat. Bur. Stand. Tech. Note 1066, 1983.

[6] T. H. Lehman, "A statistical theory of electromagnetic fields in complex cavities," EMP Interaction Note 494, 1993.

[7] D. A. Hill, "Spatial correlation function for fields in a reverberation chamber," *IEEE Trans. Electromagn. Compat.*, vol. 37, p. 138, Feb. 1995.

[8] ——, "A reflection coefficient derivation for the Q of a reverberation chamber," *IEEE Trans. Electromagn. Compat.*, vol. 38, pp. 591–592, Nov. 1996.

[9] D. A. Hill, M. L. Crawford, M. Kanda, and D. I. Wu, "Aperture coupling to a coaxial air line: Theory and experiment," *IEEE Trans. Electromagn. Compat.*, vol. 35, pp. 69–74, Feb. 1993.

[10] D. A. Hill, M. T. Ma, A. R. Ondrejka, B. F. Riddle, M. L. Crawford, and R. T. Johnk, "Aperture excitation of electrically large, lossy cavities," *IEEE Trans. Electromagn. Compat.*, vol. 36, pp. 169–178, Aug. 1994.

[11] D. A. Hill, D. G. Camell, K. H. Cavcey, and G. H. Koepke, "Radiated emissions and immunity of microstrip transmission lines: Theory and reverberation chamber measurements," *IEEE Trans. Electromagn. Compat.*, vol. 38, pp. 165–172, May 1996.

[12] J. A. Stratton, *Electromagnetic Theory*. New York: McGraw-Hill, 1941, Sec. 7.7.

[13] R. C. Wittmann and D. N. Black, "Quiet-zone evaluation using a spherical synthetic-aperture radar," in *IEEE Antennas Propagat. Soc. Int. Symp.*, Montreal, Canada, July 1997, pp. 148–151.

[14] J. M. Ladbury, G. H. Koepke, and D. G. Camell, "Evaluation of the NASA Langley Research Center mode-stirred chamber facility," Nat. Inst. Stand. Technol. Tech. Note, to be published.

[15] R. F. Harrington, *Time-Harmonic Electromagnetic Fields*. New York: McGraw-Hill, 1961.

[16] R. A. Zacharias, N. C. Ng, and T. H. Lehman, "Applying statistical electromagnetic theory to mode-stirred chamber measurements," Lawrence Livermore Nat. Lab. Rep. UCRL- ID-115667, 1993.
[17] A. Ishimaru, *Wave Propagation and Scattering in Random Media*. New York: Academic, 1978, ch. 15.
[18] E. Wolf, "New theory of radiative energy transfer in free electromagnetic fields," *Phys. Rev. D*, vol. 13, pp. 869–886, 1976.
[19] R. K. Cook, R. V. Waterhouse, R. D. Berendt, S. Edelman, and M. C. Thompson, "Measurement of correlation coefficients in reverberant sound fields," *J. Acoust. Soc. Amer.*, vol. 27, pp. 1072–1077, 1955.
[20] J. G. Kostas and B. Boverie, "Statistical model for a mode-stirred chamber," *IEEE Trans. Electromagn. Compat.*, vol. 33, pp. 366–370, Nov. 1991.
[21] J. M. Dunn, "Local, high-frequency analysis of the fields in a mode-stirred chamber," *IEEE Trans. Electromagn. Compat.*, vol. 32, pp. 53–58, Feb. 1990.
[22] D. M. Kerns, *Plane Wave Scattering-Matrix Theory of Antennas and Antenna-Antenna Interactions*. Washington, DC: U.S. Gov. Printing Office, 1981, Nat. Bur. Standards Monograph 162.
[23] C. T. Tai, "On the definition of effective aperture of antennas," *IEEE Trans. Antennas Propagat.*, vol. 9, pp. 224–225, Mar. 1961.
[24] J. Baker-Jarvis and M. Racine, "Solving differential equations by a maximum entropy-minimum norm method with applications to Fokker-Planck equations," *J. Math. Phys.*, vol. 30, pp. 1459–1463, 1989.
[25] J. N. Kapur and H. K. Kesavan, *Entropy Optimization Principles with Applications*. Boston, MA: Academic, 1992.
[26] A. Papoulis, *Probability, Random Variables, and Stochastic Processes*. New York: McGraw-Hill, 1965.

David A. Hill (M'72–SM'76–F'87) was born in Cleveland, OH, on April 21, 1942. He received the B.S.E.E. and M.S.E.E. degrees from Ohio University, Athens, in 1964 and 1966, respectively, and the Ph.D. degree in electrical engineering from Ohio State University, Columbus, in 1970.

From 1970 to 1971, he was a Visiting Fellow with the Cooperative Institute for Research in Environmental Sciences, Boulder, CO, where he worked on pulse propagation. From 1971 to 1982 he was with the Institute for Telecommunication Sciences, Boulder, CO, where he worked on antennas and propagation. Since 1982 he has been with the Electromagnetic Fields Division of the National Institute of Standards and Technology, Boulder, CO, where he works on electromagnetic theory. He is also a Professor Adjoint in the Department of Electrical and Computer Engineering of the University of Colorado, Boulder.

Dr. Hill is a member of URSI Commissions A, B, E, and F. He has served a technical editor for the IEEE TRANSACTIONS ON GEOSCIENCE AND REMOTE SENSING and the IEEE TRANSACTIONS ON ANTENNAS AND PROPAGATION.